Egyptian Journal of Petroleum (2016) 25, 221–227

HOSTED BY

ELSEVIER

Egyptian Petroleum Research Institute

Egyptian Journal of Petroleum

www.elsevier.com/locate/egyjp
www.sciencedirect.com

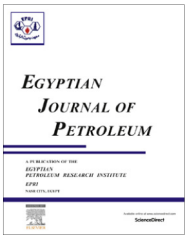

FULL LENGTH ARTICLE

Towards novel adsorptive nanomaterials: Synthesis of $Co^{2+}Mo^{6+}$ LDH for sulfur and aromatic removal from crude petrolatum

Mohsen S. Mostafa, Nermen H. Mohamed *

Petroleum Refining Division, Egyptian Petroleum Research Institute (EPRI), Nasr City, 11727 Cairo, Egypt

Received 2 April 2015; revised 13 May 2015; accepted 17 May 2015
Available online 23 December 2015

KEYWORDS

Nano-layered;
$Co/Mo(CO_3)^{2-}$-LDH;
Undesirable compounds;
Petroleum wastes;
Microcrystalline waxes

Abstract In the present work $Co/Mo(CO_3)^{2-}$-LDH material of highly energetic surface was prepared by controlled titration of ammonium carbonate and ammonium hydroxide against Co and Mo cations at elevated temperatures, while different analytical techniques were applied to proof the chemical constitution and surface features of the material as XPS (X-ray Photoelectric Spectroscopy) in addition to XRF metal analysis, FT-IR, SEM, XRD, DSC-TGA and N2 adsorption–desorption isotherm. The highly energetic surface due to formation of 4+ surface charge in the brucite layer between Co and Mo as confirmed by XPS was practically ensured when the freshly prepared $Co^{2+}Mo^{6+}$-LDH dried at 60 °C overnight without any activation has been applied as a novel adsorbent for the removal of the undesirable compounds (sulfur and aromatics compounds) from crude waxes. Suez crude petrolatum has been used during this study. Depending on the experimental data, we were successful to prepare a new type of LDHs showed high ability for removing the undesirable compounds (sulfur and aromatics) from Suez crude petrolatum. Also, in the same trend it removed low melting waxes. This leads to isolation of microcrystalline waxes from petroleum wastes which used as a lubricant, rust preventive, in the manufacture of cosmetics, and in medicine as a protective dressing, emollient, and in a lot of industrial applications.

1. Introduction

Among all the nanomaterials, LDHs may be recognized as one of the most interesting nanocandidates with a wide range of applications due to their wonderful characteristics as economy, versatility and easy methods of preparation, high surface areas, uniform compositions of sharp crystallinity, lamellar structures, high ion-exchange capacities, and memory effects.

The general formula of LDHs is expressed as $[M^{II}_{1-x}\ M^{III}_{x}(OH)_2]^{X+}\ (A^{n-})_{x/n}\ m{\cdot}H_2O$ since M^{II} represents the bivalent metals and M^{III} represents the trivalent metals, A refers to M^{II}/M^{III} molar ratio and its value is generally between 0.18 and 0.33 [1] emerging a diversity of isostructural materials, and m is the water entities intercalated and/or adsorbed to LDHs. The formation of LDH occurs as a result of the

* Corresponding author. Tel.: +20 22745902; fax: +20 22747433.
E-mail address: neremenhefiny@yahoo.com (N.H. Mohamed).

Peer review under responsibility of Egyptian Petroleum Research Institute.

http://dx.doi.org/10.1016/j.ejpe.2015.05.013

substitution of some M^{2+} cations to M^{3+} cations such that this substitution creates a positive charge ($x+$) that must be compensated with the negative charge of the interlayer anion ($A-$) and the water molecules to restore the electron neutrality of the formed structure. The positive charge created here is responsible for the intercalation of enormous numbers of organic and inorganic anions and the exchangeability of these anions to LDHs in different manners and so the responsibility to the definition of LDHs as anionic clay. In contrast to many cationic clays existing in nature as zeolites, brucite (octahedrally coordinated $Mg(OH)_2$) is the only naturally occurring LDH candidate. Based on their own features, LDHs find an extreme range of applications in different fields such as in nanoadsorbents [2–4], nanocatalysis [5,6], catalyst supports [7,8] nano hybrid organic–inorganic materials [9,10], nano polymer composites [11,12], and drug delivery [13,14].

Except LiAl-LDH of type $M^{1+}M^{3+}$ LDH, the ordinary LDHs are usually prepared from divalent and trivalent cations and there are few articles that consider the preparation of $M^{2+}M^{4+}$ LDHs [15,16] while carbonate anion is the most common interlayer anion in all types.

In lubricant oil industry, Petroleum waxes were considered as by-products during dewaxing process. Petroleum waxes were used as components of furnace residual fuel oil. Today they are available petroleum products. The petroleum waxes are classified into paraffin waxes, microcrystalline waxes and petrolatums. Petrolatum is a mineral oil jelly (i.e. petroleum jelly). It is a mixture of hydrocarbons, yellowish or whitish, gelatinous, semisolid, amorphous mass obtained from petroleum. It is used as a barrier to lock moisture in the skin in a variety of moisturizers, ointment base and also in hair care products to make your hair shine [17,18]. Refined petrolatums and microcrystalline waxes varying in properties can be produced by a selective removal of the oil and low melting waxes from petrolatum crude. The process is commonly called solvent deoiling or wax fractionation. Wax re-crystallization process is the most prevalent deoiling technique. It is sometimes called fractional crystallization technique and it is used for fractionating all types of crude waxes [18,19].

Different grades of paraffin and microcrystalline waxes have been isolated by refining of slack wax and petrolatum crudes respectively using different solvents and at the ambient fractionating temperature of 20 °C [20–22]. Many authors prepared and examined nano materials (ex. Layered double hydroxides and γ-alumina) and used the adsorption technique to remove undesirable compounds (sulfur and aromatic compounds) from crude waxes which leads to improvement in the physical properties of crude waxes [23,24].

Thus, in this study we try to prepare CoMo $(CO_3)^{2-}$-LDH by a homogeneous co-precipitation method at elevated temperatures. In this study we are trying to study the effectiveness of synthesized nano-material in the elimination of the undesirable compounds (sulfur and aromatic) from crude waxes. Furthermore, the most important is the effectiveness of synthesized nano-material in the disposal of low melting waxes from Suez crude petrolatum (solid wastes) so as to produce microcrystalline waxes in one step using different ratios (from 10 to 30 wt.%), because, it saves energy, time and does not lead to the destruction of the environment, while, traditional techniques (fractional crystallization) consume a lot of energy, time and leads to environment damage since it is done in more than one step including usage of expensive solvents and chilling.

2. Chemicals and methods

2.1. Chemicals

Anhydrous molybdenum pentachloride ($MoCl_5$) was purchased from Sigma–Aldrich (Germany), cobalt chloride hexahydrate ($CoCl_2{\cdot}6H_2O$) was purchased from El-Nasr chemical company (Egypt) and ammonium carbonate [$NH_4(CO_3)_2$] and ammonia (NH_4OH 37%) were purchased from Merck (Germany).

Suez crude petrolatum from Oil Processing Company (Marine Belayim crude) was used in this investigation for studying the efficiency of synthesized nano-layered material on removing undesired compound from crude petrolatum for separation of microcrystalline waxes.

2.2. Preparation of Co/Mo-LDH

A controlled precipitation method [25] was applied to prepare CoMo LDH by adjusting the rate of titration of ammonium carbonate and ammonium hydroxide to Co and Mo cations at elevated temperatures and controlled pH as follows. A 100 ml (60 mM) solution of $CoCl_2{\cdot}6H_2O$ and $MoCl_5$ with molar coefficient equals to 0.25 was first prepared and refluxed at 80 °C for 2 h under vigorous stirring. After, a solution of NH_4OH (20 mmol) and $NH4(CO_3)^2$ (10 mmol) was successively added to the Co and Mo cations till reaching a pH 9–10 through 6 h with the aid of a microdosing pump. The formed puffy ppt. was aged for another 12 h at the same temperature, then filtered out, washed several times till negative chloride ions ($AgNO_3$ test) and finally dried at 60 °C over night.

2.3. Material characterization

X-ray photoelectron spectroscopy XPS was conducted to investigate the Co and Mo oxidation states in the freshly prepared Co/Mo-LDH with thermo scientific XPS model K-Alpha (England). The constitution of the material with respect to Co and Mo cations was measured with X-ray fluorescence (XRF). X-ray diffraction (XRD) patterns have been recorded on a Brucker AXS-D8 Advance (Germany) of nickel-filtered copper radiation (λ = 1.5405 Å) in the region of 2 theta = 2 – 70° and speed of 8°/20 min.

The structure change of the prepared sample corresponding to a thermal treatment in the region 25–700 C was recorded with differential scanning calorimetry DSC and TGA with SDT-Q600 V20.5 Pouild 15 apparatus.

N_2 adsorption–desorption isotherms were performed with Quantachrome Nova 3200 instrument (USA) under a degassing temperature of 60 °C to conserve the parent structure of LDH where the surface area and pore volume were measured according to BET equation and BJH method respectively.

The FT-IR spectra of CoMo LDH were recorded on ATI Mattson Genesis series (KBr disk method).

Finally, scanning electron microscope (JEOL 5300 Japan) was applied to study the surface features and morphology. The lead concentration was measured with atomic absorption spectrometer (AAS) model Zeenit 700 Panalytikajena (Germany).

2.4. Physical characteristics

Suez crude petrolatum and the treated waxes were physically characterized according to American Society for Testing and Materials (ASTM) standard methods [26]. The standard methods for analysis are congealing point (ASTM D-938), refractive index (ASTM D-1747), oil content (ASTM D-721), color (ASTM D-1500) and sulfur content using X-ray fluorescence sulfur meter (ASTM D-4294).

The aromatics and n-paraffin contents were determined using liquid–solid column chromatographic technique [27–28] and GC technique, respectively. The GC apparatus used was PerkinElmer (Clarus 500), equipped with a hydrogen flame ionization detector and fused silica capillary column (60 m length × 0.32 mm i.d.), packed with poly (dimethyl siloxane) HP-1 (non-polar packing) of 0.5 m film thickness.

The classifications of isolated waxes into macro-crystalline, microcrystalline and semi-microcrystalline groups were carried out according to TAPPI-ASTM equation [29].

2.5. Adsorption process

The adsorption process was done via contacting technique which involves mixing of the wax with the activated nano-layer (until reached to 10–30 wt.% based on wax) for a definite time followed by separation of the wax and nano-layer adsorbent via centrifugation [30].

3. Results and discussion

3.1. Characterization of the adsorbent

3.1.1. XRD

It is well accepted that, layered double hydroxides or hydrotalcites have their own XRD diffraction patterns that are characterized by sharp, narrow and symmetric reflections with respect to lower 2 theta of basal planes 003, 006, and 009 followed by asymmetric and broad reflections at higher 2 theta for non-basal planes 012, 015, and 018. Fig. 1 shows the CoMo XRD pattern which obviously reflects the ultimate hydrotalcite composition of the prepared sample with the mentioned basal planes reflections. Also from Fig. 1, it can be observed that CoMo LDH has a main XRD peak at 0.68 nm which is smaller than 0.76 nm of the ordinary layered double hydroxides of M^{II}–M^{III} type, this shift can be clarified by the creation of 4+ charge between Co^{2+} and Mo^{6+} in our case rather than 1^{+} charge in the ordinary LDHs in a manner leading to stronger attraction between the CoMo LDH layers and the interlayer anion. Such decrease in the main peak basal space was first reported by Constantino and Pinnavaia [32] when they suggested the decrease of 0.76 nm value to 0.67 nm as a result of drying M2+ and M3+ LDH at 150 °C due to desorption of some interlayer water molecules.

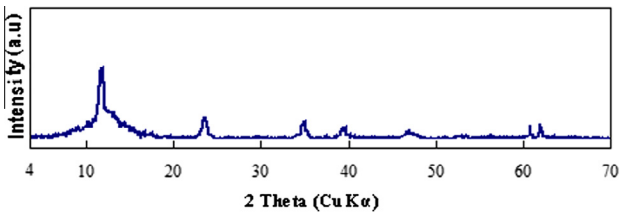

Figure 1 XRD patterns of the CoMo-LDH.

3.1.2. X-ray photoelectron spectroscopy

Fig. 2 shows the XPS analysis of CoMo LDH. From Fig. 2, it is evidenced that Mo is present in the oxidation state of 6+ since the electron binding energy of Mo (3d) is 231.90 eV, this value lays in between 231.6 and 232.7 eV related to Mo^{6+} in case of applying the same XPS for MoO_3 as standard. Here, the presence of Mo^{6+} states the preparation of Co^{2+}–Mo^{6+} LDH.

3.1.3. Elemental analysis

Generally, complete precipitation can be achieved with the homogeneous co-precipitation method specially with long aging times. According to the XRF data, the Co:Mo molar ratio is about 2.93:1 very close to 3:1 in the initial solution. The low deviation between the starting solution and the synthesized material may be due to mistakes during preparation or presence of impurities or soluble matters especially with respect to $CoCl_2{\cdot}6H_2O$; however such deviation is common in literature [31]. According to this analysis and the data given from XRD and XPS, the formula of CoMo-LDH can be written as $[Co^{2+}_{0.75}\ Mo^{6+}_{0.25}\ (OH)_2]^{0.25}\ (CO^{2-}_3)^{0.5}\ m{\cdot}H_2O$.

3.1.4. FT-IR

Fig. 3 illustrates the sample FT-IR spectra, the spectra are completely incident with those characteristic of the well known

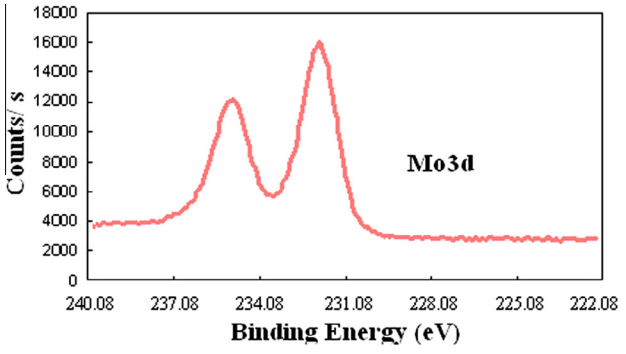

Figure 2 XPS spectra of synthesized CoMo-LD.

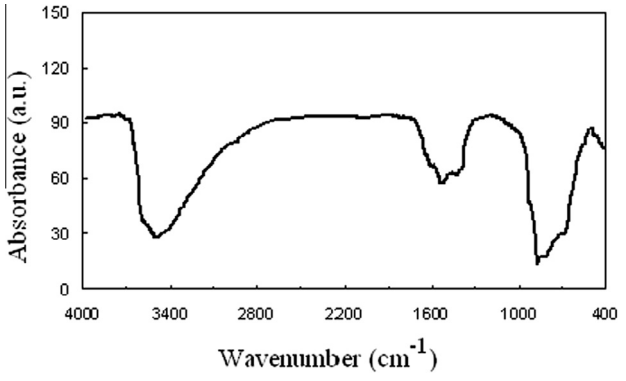

Figure 3 FT-IR spectra of the CoMo-LDH.

hydrotalcite like compounds in case of CO_3^{2-} as the interlayer anion [33]. The presence of interlamellar carbonate can be evidenced by the band observed close to 1380 cm^{-1} characteristic for the asymmetric elongation (υ3) of the CO_3^{2-} species coupled with its attendant at about 1510 cm^{-1}. This band is generally reported at 1450 cm^{-1} for free carbonate, but splits and swings on symmetry lowering which may have occurred as a result of constrained proportion inside the layers space and to the variable electrostatic actions. The broad band across the region 3600 and 3200 cm^{-1} is for the OH stretching mode created by the layer –OH groups and the interlamellar water, this broadness may be expressed as a result of the hydrogen bridges [34]. The weak shoulder at about 3000 cm^{-1} has been considered for the prolonged OH mode created by the interlamellar water molecules bonded with the interlayer anions by hydrogen bridges. The bending band of water molecules is observed as a weak band at 1600 cm^{-1} [35], while the weak bands across 1000–500 cm^{-1} region are related to the metal–metal, metal-oxide and metal hydroxide bands [36].

3.1.5. N_2 adsorption–desorption isotherm

The BET of CoMo LDH is shown in Fig. 4.The isotherm is coincident with the IV-type of IUPAC classification related to mesoporous materials [37] showing a desorption hysteresis loop blocked at virtual P/Po in between 0.4 and 0.95. The complete mesoporosity can be also realized from the isotherm since the N_2 acquisition occurred at P/Po exceeds 0.02 reflecting a full blockage of the micro pores of layered CoMo under study, this is in a good manner with the thermal treatment of the sample including drying and degassing at 60 °C to conserve its virgin structure that is fully occupied with adsorbed and interlayered water beside the bonded carbonate. The data from the isotherm are listed in Table 1 including total surface area (64.7 m^2/g), pores volume (0.163 ml g^{-1}) and pore size (10.54 nm average).

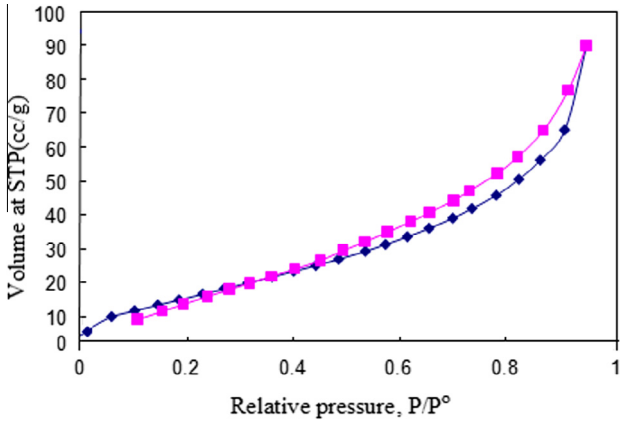

Figure 4 N2 adsorption/desorption isotherm of the CoMo-LDH.

3.1.6. Thermal analysis

Fig. 5 illustrates the thermal analysis (DSC-TGA) of CoMo layered double hydroxide. From the figure, there two weight losses at 145 °C associated with an endothermic peak at 87 °C and at 364 °C associated with its attendant endothermic peak at 365 °C. The first weight loss here is considered to be to the surface and adsorbed water removal, while the second loss is considered to be due to the destruction of the layered structure into the oxide form through removal of the interlayer carbonate and water in addition to the layer hydroxide groups. This CoMo thermograph is coincident with that of the ordinary hydrotalcites. Another result can be taken from this thermograph that it is ensuring the oxidation of Mo^{5+} under the synthesis conditions to Mo^{6+} since the thermograph shows no exothermic peaks can be related to such oxidation steps [38].

3.1.7. Scanning electron microscopy

Natural samples of layered double hydroxide (pyroaurite) exhibit plate-like morphology with plates being millimeters in thickness and centimeter in width. Also, it is known that hydrotalcite crystals possess hexagonal platy morphology if carefully crystallized.

Fig. 6 shows the SEM image of CoMo-LDH. As seen, the surface morphology of the sample is plate-like with well ordered hexagonal crystallites; this morphology is generally associated with the hydrotalcite crystallites [39,40].

3.2. Characterization of Suez crude petrolatum

3.2.1. Physico-chemical characteristics

The physical characteristics of Suez crude petrolatum as refractive index, needle penetration and kinematic viscosity increase with increasing aromatic content of Suez crude petrolatum.

The oil content is an indication of the quality of the wax. An increase in oil content results in an increase in penetration value (Table 2).

3.2.2. Molecular type composition

It is obvious from molecular type composition data (Table 2) that, Suez crude petrolatum shows very low normal paraffin content (9.32 wt.%) and high iso- and cyclo paraffin contents (56.98 wt.%). Despite the higher boiling range of Suez crude petrolatum, the congealing point is low (59 °C) as a result of the presence of high iso- and cyclo paraffin contents, which confirms the above findings.

Molecular type composition data indicate that Suez crude petrolatum has a high aromatic content (33.70 wt.%) as compared with the light and middle ones. These aromatic constituents are mainly mono-aromatic and di-aromatics (17.33 and 16.37 wt.% respectively). Data of sulfur content and color are parallel to the above findings, where the sulfur contents

Table 1 BET surface area and porosity characteristics of the CoMo-LDH.

Sample	BET area (m^2/g)	C-value in BET equation	Pores volume (ml/g)	Average pore size (nm)	Micropore volume (ml/g)
CoMo-LDH	64.7	23	0.163 ml/g	10.54	0

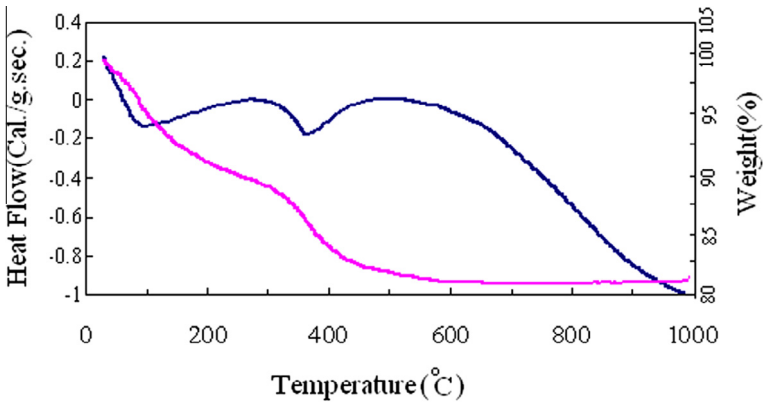

Figure 5 DSC-TGA profile of the CoMo-LDH.

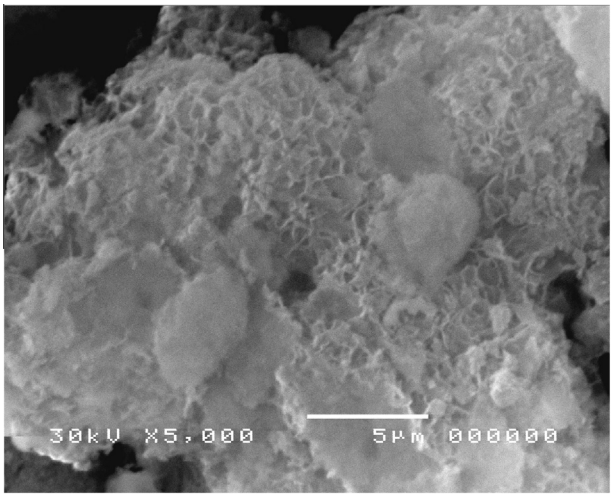

Figure 6 SEM images of CoMo-LDH.

and color values are high (1.67 wt.% and 9) respectively (Table 2).

3.3. Effect of adsorption process

The finishing process was considered the final step in refining processes. It is used to remove the undesired contaminated constituents and improve the color and color stability of the produced micro-crystalline waxes. It is clear from the data that the contacting technique has obvious effects upon the quality of the treated crude wax as its color, congealing point, mean molecular weight and penetration value are improved and accompanied by a sharp decrease in its oil content to reach 12.20, 9.55 and 5.20 wt.% by addition of 10, 20 and 30 wt.% respectively.

It can be noticed that, the wax yield decreases on increasing the ratios of nano-layer adsorbent from 10 to 30 wt.%. This may be due to the increase in surface area of nano-layer adsorbent and its high efficiency toward aromatics and low melting

Table 2 The physical characteristics and molecular type composition of Suez crude petrolatum before and after adsorption processes using CoMo-LDH.

Characteristics	Suez crude petrolatum	Crude petrolatum after adsorption		
		10 wt.%	20 wt.%	30 wt.%
Yield on crude, wt.%	100	58.20	30.55	15.22
Congealing point, °C	59	66.5	71	73
Kinematic viscosity, 98.9 °C, mm^2/s	12.75	11.90	11.00	10.89
Refractive index, 98.9 °C	1.4544	1.4480	1.4439	1.4407
Mean molecular weight	623	712	719	725
Oil content, wt.%	20.09	12.20	9.55	5.20
Needle penetration, 25 °C	203	42	30	25
Sulfur content, wt%	1.67	0.88	0.29	0.19
Color (ASTM-D 1500)	9.0	6.0	3.0	2.0
Refractive index by TAPPI-ASTM equation	–	1.4289	1.4297	1.4308
Type of wax	–	Micro-crystalline waxes		
Molecular type composition				
Total saturates, wt.%	66.30	82.98	90.00	94.20
n-Paraffin content, wt.%	9.32	13.52	15.20	20.21
Iso- and cyclo-paraffins content, wt.%	56.98	69.46	74.80	73.99
Total aromatics, wt.%	33.70	17.02	10.00	5.80
Mono aromatics, wt.%	17.33	10.85	10.00	5.80
Di-aromatics content, wt.%	16.37	6.17	0.0	0.0

waxes. This conclusion is in line with the data of congealing points and mean molecular weights of the isolated waxes which give higher values on increasing the nano-layer adsorbent ratios (Table 2).

It is clear from Table 2 that, the needle penetration decreases and the congealing point increases by decreasing the oil content of the wax by increasing the nano-layer adsorbent ratios.

Data of molecular type composition confirm the above findings as the saturate contents increase due to the decrease of the oil contents and there is a valuable decrease in the mono-aromatic constituents accompanied with the absence of di-aromatic ones for ratios 20 and 30 wt.% of nano-layer adsorbent. Data of sulfur and color are data of sulfur content and color are parallel to the above findings (Table 2).

From the above observations, it can be concluded that prepared nano-layer material is a selective adsorbent for low melting waxes and aromatics especially di-aromatic ones.

3.4. Type of isolated waxes

Table 2 indicates that the experimental refractive indices of all the waxes separated at all the addition ratios (10–30 wt.%) using CoMo-LDH as adsorbent are higher than those given by *TAPPI-ASTM* equation [41,42] and their viscosities at 98.9 °C higher than 10 centistokes, which relate these waxes to a micro-crystalline group.

4. Conclusions

The specifications for refined waxes depend on their end use which determines the degree of refining required. Refined wax is achieved by deoiling and hydrogenation or acid treatment and/or adsorption processes to satisfy the requirements of color, color stability and other specifications. Thus the waxes separated using traditional methods [21,22,43] using different solvent ratios are of more costs since, they are achieved by two processes (deoiling and hydrogenation or acid treatment and/or adsorption processes) using expensive materials. The use of prepared CoMo-LDH in deoiling Suez crude petrolatum has many benefits:

1. Elimination the deoiling solvent ratio, which is better in plant design and cost conservation.
2. Eliminates the recrystallization step of the waxes.

Thus such application is cost effective.

Acknowledgements

The work is sponsored by the Egyptian Petroleum Research Institute (EPRI) Cairo, Egypt.

References

[1] S.J. Palmer, R.L. Frost, Ind. Eng. Chem. Res. 49 (2010) 8969–8976.
[2] B. Tamás, P. Ágnes, G. Zoltán, D. Imre, Appl. Clay Sci. 44 (2009) 75–82.
[3] Y. Yiqiong, G. Naiyun, D. Yang, Z. Shiqing, Appl. Clay Sci. 65–66 (2012) 80–86.
[4] F. Brunaa, R. Celis, I. Pavlovic, C. Barrigaa, J. Cornejob, M.A. Ulibarri, J. Hazard. Mater. 168 (2009) 1476.
[5] R. Andrey, H. Vasile, T. Didier, L. Catherine, A. Didier, C. Bernard, T. Philippe, Appl. Catal. A 397 (2011) 218–224.
[6] P.X. Zhi, Z. Jia, O.A. Moses, Z. Hong, Z. Chunhui, Appl. Clay Sci. 53 (2011) 139–150.
[7] H. Fu-An, Z. Li-Ming, J. Colloid Interface Sci. 315 (2007) 439–444.
[8] K. František, J. Květa, Appl. Clay Sci. 53 (2011) 305–316.
[9] S. Hidouria, Z.M. Baccara, H. Abdelmelek, T. Noguerd, J.-L. Martyd, M. Campàsc, Talanta 85 (2011) 1882–1887.
[10] P.X. Zhi, S.B. Paul, Appl. Clay Sci. 48 (2010) 235–242.
[11] Q. Longzhen, Q. Baojun, J. Colloid Interface Sci. 301 (2006) 347–351.
[12] L. Fabrice, I. Abdallah, V. Vincent, J. Colloid Interface Sci. 332 (2009) 327–335.
[13] W. Yunyi, M. Kathryn, P.X. Zhi, C. Min, Q.L. Gao, F.B. Perry, M.C. Helen, Biomaterials 31 (2010) 8770–8779.
[14] V. Rives, M. Del Arco, C. Martín, J. Controlled Release 169 (2013) 28–39.
[15] X. Sheng-Jie, L. Feng-Xian, N. Zhe-Ming, S. Wei, X. Ji-Long, Q.C. Ping-Ping, Appl. Catal. B 144 (2014) 570–579.
[16] M.S. Elena, P. Eveline, M. Mirjam, G.V. Tendeloo, C. Pegie, F. V. Etienne, Microporous Mesoporous Mater. 111 (2008) 12–17.
[17] W.M. Mazee, in: G.D. Hobson (Ed.), Modern Petroleum Technology, fourth ed., Applied Science Publishers Ltd, on behalf of the Institute of Petroleum, Great Britain, 1973.
[18] A. Sequeria Jr., Lubricant Base Oil and Wax Processing, Marcel Dekker Inc., New York, 1994, pp. 17–41.
[19] F. Richter, in: G. Alan (Ed.), Modern Petroleum Technology, Vol. 2, Lucas, John Wiley and sons Ltd., on behalf of the Institute of Petroleum, New York, 2000.
[20] N.H. Mohamed, M.T. Zaky, A.S. Farag, A.F.M. Fahmy, Pet. Sci. Technol. 26 (2008) 562–574.
[21] M.T. Zaky, N.H. Mohamed, J. Taiwan Inst. Chem. Eng. 41 (4) (2010) 360–366.
[22] N.H. Mohamed, M.T. Zaky, A.S. Farag, Fuel Process. Technol. 92 (2011) 2024–2029.
[23] O. Saber, N.H. Mohamed, A.A. Al, Jaafari, Fuel Process. Technol. 92 (2011) 946–951.
[24] M.T. Zaki, N.H. Mohamed, I.N. Maher, H. Mamdouh, Fuel Process. Technol. 106 (2013) 625–630.
[25] F. Cavani, F. Trifiro, A. Vaccari, Catal. Today 11 (1991) 173–301.
[26] Annual Book of ASTM-Standards (American Society for Testing and Materials), Petroleum Products, Lubrications, West Conshohocken, 1999. Sect. 5.
[27] L.R. Snyder, in: E. Heftmann (Ed.), Chromatography, Van Nostrand Reinhold Company, New York, 1975.
[28] B.J. Mair, F.D. Rossini, ASTM Spec. Tech. Publ. 224 (1958) 9–46.
[29] Concawe, Petroleum Waxes and Related Products, p.1, Concawe, Brussels, Report No. 99/110, December 1999.
[30] N.H. Mohamed, M.T. Zaky, Pet. Sci. Technol. 22 (2004) 1553–1569.
[31] M. Intissar, R. Segni, C. Payen, J. Besse, F. Leroux, J. Solid State Chem. 167 (2002) 508–516.
[32] V.R.L. Constantino, T. Pinnavaia, Inorg. Chem. 34 (1995) 883–892.
[33] J.T. Kloprogge, R.L. Frost, J. Solid State Chem. 146 (1999) 506–515.
[34] F.M. Labajos, V. Rives, M.A. Ulibarri, J. Mater. Sci. 27 (1992) 1546–1552.
[35] J. Perez-Ramireez, G. Mul, F. Kapteijn, J.A. Moulijn, J. Mater. Chem. 11 (2001) 821–830.
[36] A.M. El-Toni, S. Yin, T. Sato, Mater. Chem. Phys. 89 (2005) 154–158.

[37] G. Wu, X. Wang, B. Chen, J. Li, N. Zhao, W. Wei, Y. Sun, Appl. Catal. A 329 (2007) 106–111.
[38] S. Miyata, Clays Clay Miner. 23 (1975) 369–375.
[39] H. Hansen, C. Koch, Appl. Clay Sci. 10 (1995) 5–19.
[40] M. Ogawa, Sh. Asai, Chem. Mater. 12 (2000) 3253.
[41] S.W. Ferris, Petroleum Waxes, Characterization, Performance and Additives, Technical Association of the Pulp and Paper Industry, STAP, 2, Special Technical Association Publication, New York, 1963, pp. 1–19.
[42] R.I. Gottshall, C.F. McCue, in: J.P. Allinson (Ed.), Criteria for Quality of Petroleum Products, Applied Science Publishers Ltd., London, 1973, pp. 209–225.
[43] N.H. Mohamed, Fuel Process. Technol. 96 (2012) 116–122.